Magnetic Switch of Permeability for Polyelectrolyte Microcapsules Embedded with Co@Au Nanoparticles

Zonghuan Lu,[†] Malcolm D. Prouty,[†] Zhanhu Guo,[‡] Vladimir O. Golub,[§] Challa S. S. R. Kumar,*[,‡] and Yuri M. Lvov*[,†]

Institute for Micromanufacturing, Louisiana Tech University, Ruston, Louisiana; Center for Advanced Microstructures & Devices, Louisiana State University, Baton Rouge, Louisiana; and Institute of Magnetism, National Academy of Sciences of Ukraine, Kiev, Ukraine

Received September 23, 2004. In Final Form: November 24, 2004

We explored using a magnetic field to modulate the permeability of polyelectrolyte microcapsules prepared by layer-by-layer self-assembly. Ferromagnetic gold-coated cobalt (Co@Au) nanoparticles (3 nm diameter) were embedded inside the capsule walls. The final 5 μm diameter microcapsules had wall structures consisting of 4 bilayers of poly(sodium styrene sulfonate)/poly(allylamine hydrochloride) (PSS/PAH), 1 layer of Co@Au, and 5 bilayers of PSS/PAH. External alternating magnetic fields of 100−300 Hz and 1200 Oe were applied to rotate the embedded Co@Au nanoparticles, which subsequently disturbed and distorted the capsule wall and drastically increased its permeability to macromolecules like FITC-labeled dextran. The capsule permeability change was estimated by taking the capsule interior and exterior fluorescent intensity ratio using confocal laser scanning microscopy. Capsules with 1 layer of Co@Au nanoparticles and 10 polyelectrolyte bilayers are optimal for magnetically controlling permeability. A theoretical explanation was proposed for the permeability control mechanisms. "Switching on" of these microcapsules using a magnetic field makes this method a good candidate for controlled drug delivery in biomedical applications.

Introduction

Layer-by-layer (LbL) assembly can construct an ultrathin film via alternate adsorption of oppositely charged polyions, nanoparticles, and biomolecules.[1] The obtained films have thicknesses in the nanometer range and tunable properties to their surroundings, such as permeability, solubility, and morphology.[1] The development of polyelectrolyte microcapsules is based on LbL assembly on nano- or microscale cores, for instance, cells and inorganic or organic particles, including drugs, which have recently gained intensive attention.[2−4] Cores, with diameters ranging from nanometers to microns, are coated with alternating layers of linear polycations, polyanions, and other materials. After dissolving the cores, hollow microcapsules were gained with ordered walls of needed composition and thicknesses in the range of 20−100 nm. The capsules have tunable permeability for molecules of different sizes on the basis of open-and-close mechanisms by adjusting the environmental stimuli.[5−8] These capsules offer broad perspectives in encapsulation, transport, and controllable delivery of drugs, minerals, and proteins. Changing the pH value of solutions induces the formation of tiny pores in the nanometer range, which allows macromolecules to pass through the capsule walls;[6] adjusting solution ionic strength or adding organic solvent will also influence permeability.[7,8] These permeability controls are achieved by changing the charge densities of linear polyelectrolytes, which results in relaxing the capsule walls. However, the austere conditions of these methods limit the utilization of them in the biomedical field for controlled drug delivery applications because they are often not consistent with physiological conditions that occur within the human body.

Another promising way to achieve permeability control is to embed ferromagnetic nanoparticles into capsule walls. The capsules might be modulated by an external oscillating magnetic field to control the permeability when needed and thus control the release of the substances in the capsules. Numerous studies have been conducted on applying magnetic particles to treat human diseases, such as cancer.[9−13] A new concept for targeted as well as

[†] Louisiana Tech University.
[‡] Louisiana State University.
[§] National Academy of Sciences of Ukraine.

(1) (a) Decher, G. *Science* **1997**, *277*, 1232. (b) Yoo, D.; Shiratori, S.; Rubner, M. *Macromolecules* **1998**, *31*, 4309−4318. (c) Schlenoff, J. B.; Dubas, S. T. *Macromolecules* **2001**, *34*, 139−160. (d) Harris, J. J.; Stair, J. L.; Bruening, M. L. *Chem. Mater.* **2000**, *12*, 1941−1946. (e) Lvov, Y.; Lu, Z.; Zu, X.; Schenkman, J.; Rusling, J. *J. Am. Chem. Soc.* **1998**, *120*, 4073−4080.

(2) (a) Donath, E.; Sukhorukov, G. B.; Caruso, F.; Davis, S. A.; Möhwald, H.; *Angew. Chem., Int. Ed.* **1998**, *37*, 2201−2205. (b) Sukhorukov, G. In *Novel Methods to Study Interfacial Layers*; Möbius, D., Miller, R., Eds.; Elsevier: Amsterdam, 2001; pp 384−415. (c) Antipov, A. A.; Sukhorukov, G. B.; Fedutik, Y. A.; Hartmann, J.; Giersig, M.; Möhwald, H. *Langmuir*, **2002**, *18*, 6687−6693.

(3) (a) Lbarz, G.; Dahne, L.; Donath, E.; Möhwald, H. *Adv. Mater.* **2001**, *13*, 1324−1327. (b) Dahne, L.; Leporatti, S.; Donath, E.; Möhwald, H. *J. Am. Chem. Soc.* **2001**, *123*, 5431−5436.

(4) (a) Ai, H.; Fang, M.; Jones, S.; Lvov, Y. *Biomacromolecules* **2002**, *3*, 560−564. (b) Ai, H.; Jones, S.; De Villiers, M.; Lvov, J. *J. Controlled Release* **2003**, *86*, 54−60.

(5) (a) Mendelson, J.; Barrett, C.; Chan, V.; Pal, A.; Mayes, A.; Rubner, M.; *Langmuir* **2000**, *16*, 5017. (b) Antipov, A. A.; Sukhorukov, G. B.; Leporatti, S.; Radtchenko, I. L.; Donath, E.; Möhwald, H. *Colloids Surf., A* **2002**, *198−200*, 535−541.

(6) (a) Tiourina, O. P.; Antipov, A. A.; Sukhorukov, G. B.; Larionova, N. I.; Lvov, Y.; Möhwald, H. *Macromol. Biosci.* **2001**, *1*, 209−214. (b) Sukhorukov, G. B.; Antipov, A. A.; Voigt, A.; Donath, E.; Möhwald, H. *Macromol. Rapid Commun.* **2001**, *22*, 44−46.

(7) Antipov, A. A.; Sukhorukov, G. B.; Möhwald, H. *Langmuir* **2003**, *19*, 2444−2448.

(8) (a) Lvov, Y.; Antipov, A.; Mamedov, A.; Möhwald, H.; Sukhoruhov, G. B. *Nano Lett.* **2001**, *1*, 125−128. (b) Radtchenko, I. L.; Sukhorukov, G. B.; Möhwald, H. *Int. J. Pharm.* **2002**, *242*, 219−223.

(9) (a) Rosensweig, R. E. *J. Magn. Magn. Mater.* **2002**, *252*, 370−374. (b) Hergt, R.; Andra, W.; D'Ambly, C. G.; Hilger, I. *IEEE Trans. Magn.* **1998**, *34*, 3745−3754.

(10) Grob, C.; Buscher, K.; Romanus, E.; Helm, C. A.; Weitschies, W. *Eur. Cells Mater.* **2002**, *3*, 163−166.

(11) Babincova, M.; Cicmanec, P.; Altanerova, V.; Altaner, C.; Babinec, P.; *Bioelectrochemistry* **2002**, *55*, 17−19.

(12) (a) Saslawski, O.; Weingarten, C.; Benoit, J. P.; Couvreur, P. *Life Sci.* **1988**, *42*, 1521−1528. (b) Kost, J.; Wolfrum, J.; Langer, R. *J. Biomed. Mater. Res.* **1987**, *21*, 1367−1373.

10.1021/la047629q CCC: $30.25
Published on Web 00/00/0000 PAGE EST: 8.1

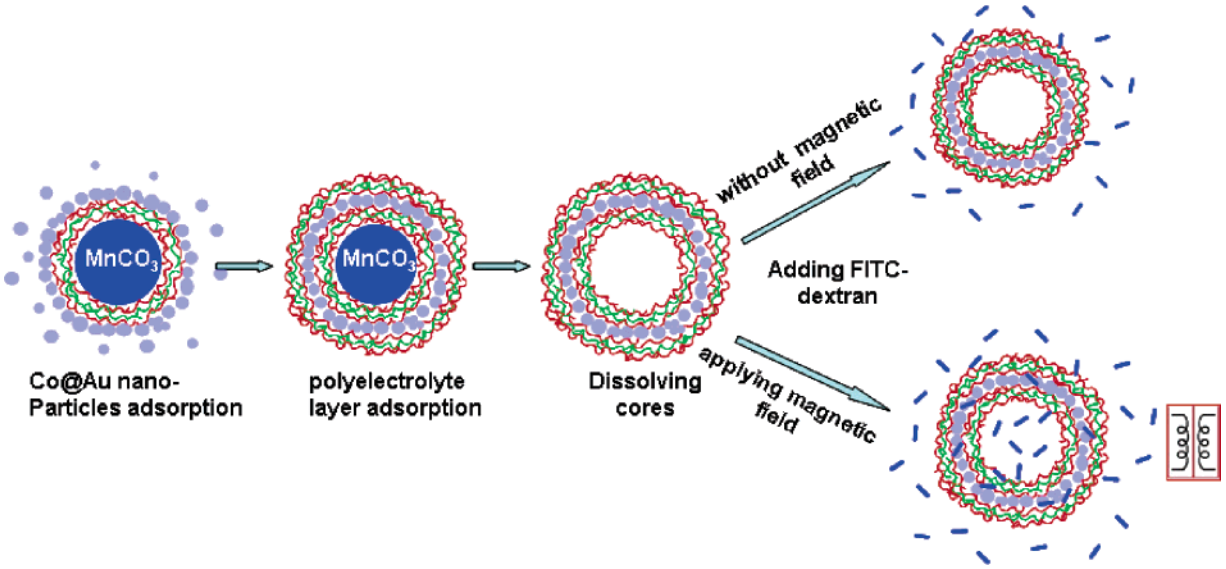

Figure 1. Scheme of the assembly and permeability test for microcapsules embedded with Co@Au nanoparticles under an oscillating magnetic field.

controlled release of anticancer drugs, using magnetic nanoparticles within a polymeric shell, has been recently proposed.[14] The magnetic fluid hyperthermia (MFH) method applies a high-frequency alternating magnetic field to heat superparamagnetic nanoparticles localized in a tumor to destroy diseased cells without damaging healthy tissue.[9,10] Magnetic particles, with diameters ranging from nanometers to millimeters, were also studied to be embedded inside alginate or liposome matrixes combined with drugs and tested for their controllable drug release behavior using a low-frequency external magnetic field.[11,12] Magnetic particles of interest include magnetite, strontium ferrite, manganese ferrite, and others.[10,13b] However, up to now, there is no study about embedding magnetic nanoparticles into walls of hollow capsules, thereby modulating the permeability and release behavior of the capsules. In this work, ferromagnetic cobalt nanoparticles coated with gold shells (Co@Au nanoparticles) were embedded into polyelectrolyte capsules fabricated with layer-by-layer assembly of poly(sodium 4-styrene sulfonate) and poly(allylamine hydrochloride) (Figure 1). Application of low-frequency alternating magnetic fields to such magnetic capsules resulted in an increase of their wall permeability; therefore, external magnetic fields may "switch on" unloading of these microcapsules.

Experimental Section

Materials. Poly(sodium 4-styrene sulfonate) (PSS, MW 70 000), poly(allylamine hydrochloride) (PAH, MW 70 000), and poly(diallyldimethylammonium chloride) (PDDA, MW 1 000 000) were used for LbL assembly. Fluorescein isothiocyanate (FITC) and rhodamine B isothiocyanate (RBITC) were used to label dextran and PAH, respectively, following the procedure described in ref 2c, which helps with capsule visualization under confocal laser scanning microscopy (CLSM). FITC−dextran (MW 2 000 000) was used for capsule permeability tests. Cobalt chloride (anhydrous, beads, 99.99%, packaged under argon in ampules), potassium tetrachloroaurate(III) (99.999%), tetrahydrofuran (THF, 99.9%, inhibitor free, packaged under nitrogen), lithium hydrotriethyl borate (superhydride) as 1 M solution in THF, dodecyldimethyl (3-sulfopropyl) ammonium hydroxide (SB12), and ethanol (reagent grade, anhydrous, water < 0.003%) were used for the synthesis of Co@Au nanoparticles. All the chemicals were purchased from Sigma-Aldrich and used without further treatments.

Co@Au Nanoparticle Fabrication and Characterization. The Co@Au nanoparticles were fabricated using a chemical reduction method.[23] The Co particles were fabricated using 3-(*N*,*N*-dimethyldodecylammonio) propanesulfonate (SB12) as the surfactant to prevent agglomeration and lithium hydrotriethyl borate (LiBEt3H, superhydride) as the reducing agent. To prevent Co nanoparticles from oxidization, a novel gold shell was formed around the Co particles by a displacement method in THF (tetrahydrofuran) media based on the following reaction:[21]

$$KAuCl_4 + Co_x\text{-SB12} \rightarrow \textbf{Co@Au}\text{-SB12} + KCl$$

In a typical procedure, the precursor cobalt nanoparticles were added to 50 mL $KAuCl_4$ (0.024 M) in THF solution under untrasonication and inert atmospheric conditions. The initially

(13) (a) Ruuge, E. K.; Rusetski, A. N. *J. Magn. Magn. Mater.* **1993**, *122*, 335−339. (b) Wilhelm, C.; Billotey, C.; Roger, J.; Pons, J. N.; Bacri, J. C.; Gazeau, F. *Biomaterials* **2001**, *24*, 1001−1011.

(14) (a) Kumar, C. S. S. R.; Leuschner, C.; William, H.; Hormes, J. Magnetic Nanoparticles for Therapy and Diagnosis. U.S. Patent Application (US 10/816,732), 2004. (b) Kumar, C. S. S.; Leuschner, C.; Doomes, E. E.; Henry, L. L.; Juban, M.; Hormes, J. *J. Nanosci. Nanotechnol.* **2004**, *4*, 245−249.

(15) Antipov, A. A.; Shchukin, D.; Fedutik, Y.; Petrov, A. I.; Sukhorukov, G. B.; Möhwald, H. *Colloids Surf., A* **2003**, *224*, 175−183.

(16) Lvov, Y.; Ariga, K.; Ichinose, I.; Kunitake, T. *J. Am. Chem. Soc.* **1995**, *117*, 6117−6122.

(17) Leporatti, S.; Gao, C.; Voigt, A.; Donath, E.; Möhwald, H. *Eur. Phys. J.* **2001**, *E5*, 13−20.

(18) Fang, M.; Grant, P.; McShane, M.; Sukhorukov, G.; Golub, V.; Lvov, Y. *Langmuir* **2002**, *18*, 6338−6344.

(19) Golub, V.; Kakazei, N.; Kravets, A.; Lesnik, N.; Pogorelov, Y.; Sousa, J.; Vovk, A. *Mater. Sci. Forum* **2001**, *197*, 373−376.

(20) Shchukin, D.; Shutava, T.; Sukhorukov, G.; Lvov, Y. *Chem. Mater.* **2004**, *16*, 3446−3451.

(21) (a) Bonnemann, H.; Brijoux, W.; Joussen, T. *Angew. Chem., Int. Ed. Engl.* **1990**, *29*, 273−274. (b) Guo, Z.; Kumar, C. S. S. R.; Henry, L. L.; Hormes, J.; Podlaha, E. J. Electroless Method to Fabricate Core−shell Nanoparticles. Abstracts, 205th Meeting of The Electrochemical Society, San Antonio, TX, May 9−13, 2004. (c) Guo, Z.; Kumar, C. S. S.; Henry, L. L.; Doomes, E. E.; Hormes, J.; Podlaha-Murphy, E. J. *J. Electrochem. Soc.* **2005**, *152*, D1−D5. (d) Shon, Y.; Dawson, G. B.; Porter, M.; Murray, R. W. *Langmuir* **2002**, *18*, 3880−3885. (e) Huang, T.; Murray. R. W. *J. Phys. Chem. B* **2003**, *107*, 7434−7440.

(22) (a) Salazar-Alvarez, G.; Mikhailova, M.; Toprak, M.; Zhang, Y.; Muhammed, M. *Mater. Res. Soc. Symp. Proc.* **2002**, *707* (Self-Assembly Processes in Materials), 263−268. (b) Petit, C.; Pileni, M. P. *J. Magn. Magn. Mater.* **1997**, *166*, 82−90. (c) Cliffel, D. E.; Zamborini, F. P.; Gross, S. M.; Murray, R. W. *Langmuir* **2000**, *16*, 9699−9702.

(23) Guo, Z.; Kumar, C. S. S. R.; Henry, L. L.; Saw, C. K.; Hormes, J.; Podlaha, E. J. 49th Magnetism and Magnetic Materials (MMM) Annual Conference Proceedings, 2004, p 366.

brown solution changed to blue, indicating that the gold ions oxidized the cobalt surface atoms on the cobalt nanoparticles. The reaction was continued for an additional 1 h, and the core−shell nanoparticles were washed thoroughly with THF and dried under vacuum. The resulting nanoparticles were characterized using transmission electron microscopy (TEM, JEOL 2010) with an accelerated voltage of 200 kV and a zeta potential analyzer (Zeta Plus, Brookhaven Instruments Corp.).

Co@Au nanoparticles were tested using a SQUID magnetometer (Quantum Design Inc., model MPMS 5S) to analyze the magnetic properties of the nanoparticles. The samples for magnetic measurements were prepared in powder form in gelatin capsules. The temperature-dependent magnetization process was investigated using the zero field cooled (ZFC) and field cooled (FC) methods.[23] ZFC was done by cooling the sample first to 4 K without a field; then magnetization changes were recorded with the temperature increasing from 4 to 300 K with an applied field of 100 Oe. FC was recorded immediately after ZFC by decreasing the temperature from 300 to 4 K with a constant field of 100 Oe. Field-dependent magnetization was tested for two temperatures: 10 and 300 K. To test the oxidative stability of the cobalt cores, both the zero field cooled and field cooled methods, with an applied field of 30 kOe at 10 K, were recorded.

Capsule Preparation. Hollow polyelectrolyte microcapsules were prepared using manganese carbonate cores[15] with an average core diameter of about 5.5 μm. First, 200 μL negatively charged PSS solution and positively charged PAH solution, with concentrations of 2 mg/mL, were absorbed alternatingly on cores in 10 mL, 1 mg/mL $MnCO_3$ core aqueous suspensions. For each polyelectrolyte layer, washing with deionized (DI) water three times was carried out to remove excess polyelectrolytes after a 15 min absorption period. Layer forming continued until four bilayers of PSS and PAH were absorbed on the cores. Then, after another layer of PSS was adsorbed, 500 μL of 1.2 mg/mL Co@Au nanoparticle solution was added into the $MnCO_3$ core suspension. After a 30 min adsorption period, the cores with adsorbed Co@Au nanoparticles were washed three times using DI water, and the $MnCO_3$ cores with adsorbed Co@Au nanoparticles were separated from the free (unabsorbed) nanoparticles in the solution by the precipitation method. The free nanoparticles precipitate much slower than the cores with nanoparticles adsorbed. Four to eight PSS/PAH bilayers were assembled to wrap up the nanoparticles sequentially after the desired number of Co@Au layers were coated on the $MnCO_3$ cores. The assembly of layers can be confirmed by zeta potential changes of the core surface and quartz crystal microbalance (QCM) resonance frequency changes (USI-Systems, Japan).

The manganese carbonate cores were dissolved using 0.1 M EDTA disodium salt solution at a pH of about 4.5 for 3−4 h.[15] After dissolving, the capsules obtained were centrifuged and washed using DI water three to four times and stored in DI water.

Capsule Permeability Test. Hollow capsules were washed using pH 7.5, 0.02 M Tris buffer three times and then kept in the same buffer overnight to ensure the capsules are in a close state.[5b,6] CLSM was used to check the permeability of capsules to macromolecules before and after applying alternating magnetic fields. FITC−dextran, with a molecular weight of 2 000 000, was used as a fluorescence indicator for diffusion tests. An alternating electromagnetic field, with frequencies ranging from 20 to 2000 Hz and a magnetic induction of 1200 Oe, was applied to oscillate and disturb the Co@Au nanoparticles embedded inside the capsule walls. The magnetic capsules were kept inside the alternating magnetic field for 5−30 min before checking the permeability change of their walls. The ratio of fluorescence intensities inside and outside of the capsules was selected as a measurement for the capsule permeability change. It is considered in this paper that the capsules are impermeable if the fluorescence intensity inside the capsules is 0.5 ($I/I_0 = 0.5$, where I is the internal fluorescence intensity inside the capsules, and I_0 is the external intensity outside the capsules) less than that outside of the capsules after adding fluorescence dye for 15 min.

Capsule Characterization. Two kinds of capsules were checked using scanning electron microscopy (SEM, AMRAY 1830): capsules with and without embedded Co@Au nanoparticles. Samples were prepared by drying capsules on 1 × 1 cm silicon wafers. After drying, platinum sputtering was used to apply an ultrathin metal layer (∼0.5 nm) to enhance the image quality taken in the experiments.

CLSM and atomic force microscopy were used to investigate the size, morphology, and structure of hollow microcapsules embedded with Co@Au nanoparticles and capsule permeability changes before and after applying an alternating magnetic field. For microcapsule checking with atomic force microscopy (AFM), the Q-Scope 250 Quesant instrument with intermittent-contact mode was used. The samples were prepared by adding about 10 μL nanoparticle suspensions on a 1.5 × 1.5 cm mica slide and dried for 24 h before checking. To allow CLSM to check the capsules and their loading, the capsules were fabricated using RBITC-labeled PAH, and fluorescent FITC−dextran (MW 2 000 000) was used as the macromolecule for the permeability tests. Before applying an alternating magnetic field, 20 μL capsule suspensions were mixed with 20 μL FITC−dextran solution (0.5 mg/mL, pH 7.5) and checked by CLSM for fluorescence intensity changes inside the capsules every 5 min up to 1 h. Then, 50 μL capsule suspensions were mixed with 50 μL FITC−dextran solution. The mixture was put in an alternating magnetic field, and the fluorescence intensity was checked every 5 min. The solution pH values were kept at 7.5 all the time during the experiments. The instrument used in this work is a confocal laser scanning microscope (Leica-SP2, Germany) with a 63× oil immersion objective.

Results and Discussion

Co@Au Nanoparticle Characterization. Figure 2a shows the UV−vis spectrum of Co@Au core−shell nanoparticles in ethanol solution. The presence of an absorption peak at 585 nm due to the gold plasmon resonance is indicative of the formation of a Au shell around the cobalt nanoparticles. It was reported that the Co nanoparticles have no plasmon resonance peak at the UV region.[22] A large red shift of the plasmon absorption, when compared with that of pure gold nanoparticles (∼530 nm),[22c] could be attributed to the presence of a cobalt core and also indicate that almost no free gold nanoparticles were formed in the displacement reaction, which is consistent with the literature report on gold-coated silver nanoparticles.[25] Such a shift was previously noticed for gold-coated γ-Fe_2O_3 core−shell nanoparticles, gold-coated silver nanoparticles, and a silver shell around a silica core.[24,25]

Figure 2b shows a TEM bright-field micrograph of the Co@Au core−shell nanoparticles. The nanoparticles were found to be nearly monodisperse with a diameter of 2.7 nm ± 0.5 nm (the diameter was calculated using Scion software from Scion Corp. for counting more than 150 nanoparticles). The image contrast, which is directly related to differences in the atomic number or projected specimen mass thickness, has been used as a distinguishing criterion for the core−shell structure.[26] The high-resolution TEM (HRTEM) image in Figure 2b (inset) shows the contrast difference between the cobalt core and the gold shell. It can be inferred from the HRTEM image that even though the thickness of the gold shell around the cobalt core was not uniform, it appeared to completely coat the cobalt core. The formation of a more spherical shell, rather than other shapes, is due to its lower surface energy compared with other shapes, or the Ostwald ripening process.[25] The gold shell thickness was also

(24) Cliffel, D. E.; Zamborini, F. P.; Gross, S. M.; Murray, R. W. *Langmuir* **2000**, *25*, 9699−9702.
(25) (a) Sun, Y.; Mayers, B. T.; Xia, Y. *Nano Lett.* **2002**, *2*, 481−485. (b) Sun, Y.; Xia, Y. *Nano Lett.* **2003**, *3*, 1569−1572. (c) Jackson, J. B.; Halas, N. J. *J. Phys. Chem. B* **2001**, *105*, 2743.
(26) (a) Fang, J.; He, J.; Shin, E. Y.; Grimm, D.; O'Connor, C. J.; Jun, M. *Mater. Res. Soc. Symp. Proc.* **2003**, *774* (Materials Inspired by Biology), 149−154. (b) Lal, S.; Westcott, S. L.; Taylor, R. N.; Jackson, J. B.; Nordlander, P.; Halas, N. J. *J. Phys. Chem. B* **2002**, *106*, 5609−5612. (c) Jackson, J. B.; Halas, N. J. *J. Phys. Chem. B* **2001**, *105*, 2743−2746.

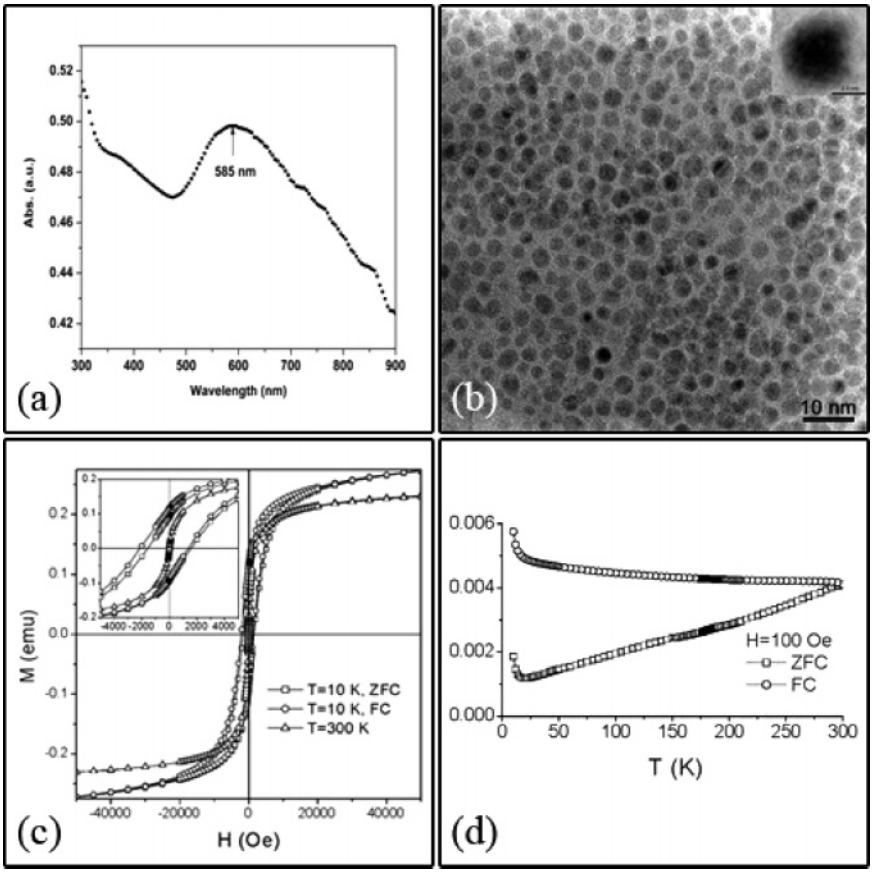

Figure 2. (a) UV/vis spectrum and (b) TEM and HRTEM (inset) images of Co@Au nanoparticles (instruments used: UV/vis, Thermo Spectronic, model Genesys 10-S; TEM, JEOL 2010). (c) Hysteresis loops of the Co@Au nanoparticles recorded in ZFC mode at 300 and 10 K and FC (H = 30 kOe) mode at 10 K (ref 23). (d) The temperature dependences of the magnetic moment measured in ZFC and FC modes for the Co@Au nanoparticles.

estimated based on the weight percentage of gold in the core−shell nanoparticles (Au wt % = 38.1, determined from atomic absorption analysis) and the particle size from TEM, assuming bulk density and standard spherical shape with symmetric structure. The thickness of the shell was calculated to be 0.7 nm, which is in agreement with the value obtained from the HRTEM image.

The blocking temperature (T_B), determined at the maximum of the ZFC curve, characterizes the transition temperature between the superparamagnetic state and the ferromagnetic state. At temperatures below the blocking temperature, materials show ferromagnetic properties, whereas at temperatures above the blocking temperature, materials show paramagnetic properties, otherwise known as superparamagnetism. The blocking temperature for Co@Au nanoparticles is above room temperature (Figure 2d), unlike the blocking temperature for the precursor pure cobalt nanoparticles (124.0 K, superparamagnetic), indicating that the core−shell nanoparticles are ferromagnetic.[23] The coercivity of a hysteresis loop is the strength of a magnetic field needed to reduce the magnetization of a ferromagnetic material to zero after it has reached saturation.[27a] A hysteresis observed at room temperature is a direct confirmation of the ferromagnetic nature of the Co@Au nanoparticles. The reason for the ferromagnetic nature of the Co@Au nanoparticles will be discussed later.

(27) (a) Mizukoshi, Y.; Fujimoto, T.; Nagata, Y.; Oshima, R.; Maeda, Y. *J. Phys. Chem. B* **2000**, *104*, 6028−6032. (b) Murray, C. B.; Sun, S. H.; Gaschler, W.; Doyle, H.; Betley, T. A.; Kagan, C. R. *IBM J. Res. Dev.* **2001**, *45*, 47−56. (c) Teng, X.; Yang, H. *J. Am. Chem. Soc.* **2003**, *125*, 14559−14563.

Layer-by-Layer Assembly on QCM Electrode and Microcores. Co@Au nanoparticles (DI water, pH ~ 7.0) were first checked using zeta potential analysis; the obtained surface potential is +15 ± 5 mV for different nanoparticle batches. That indicates the surface charges of the nanoparticles are positive, so negatively charged PSS was selected to assemble alternatingly with the Co@Au nanoparticles.

First, we elaborated the assembly conditions on QCM resonators monitoring the process by the weight addition on every deposition cycle. Two bilayers of PSS/PDDA were used as precursor layers. The results are shown in Figure 3a. The plot shows a stable growth of nanoparticle layers on the QCM resonator. From the QCM frequency shift plot, one can see formation of the multilayer corresponding to the planned composition of microcapsule walls: first, a four-step precursor layer, and then three bilayers of nanoparticles and PSS. Considering the Co density of 8.7 g/cm^3 and a particle packing coefficient of ca. 52%, the estimated monolayer thickness for Co@Au nanoparticles is ca. 4−6 nm. Here, each nanoparticle in the monolayer (the nanoparticles were considered to form a monolayer on the surface of the resonator with a simple cubic (SC) structure) was considered as a sphere, which occupies 52% of a cubic structure as shown in the following formulation: $4\pi r^3/3a^3 = 4\pi a^3/a^3 2^3 = 4\pi/24 \approx 0.52$, where a is the length of the cube and r is the radius of the sphere ($r = a/2$). This is just an estimated value. This thickness was obtained from the corresponding frequency shift using the Sauerbrey equation supported with experimental

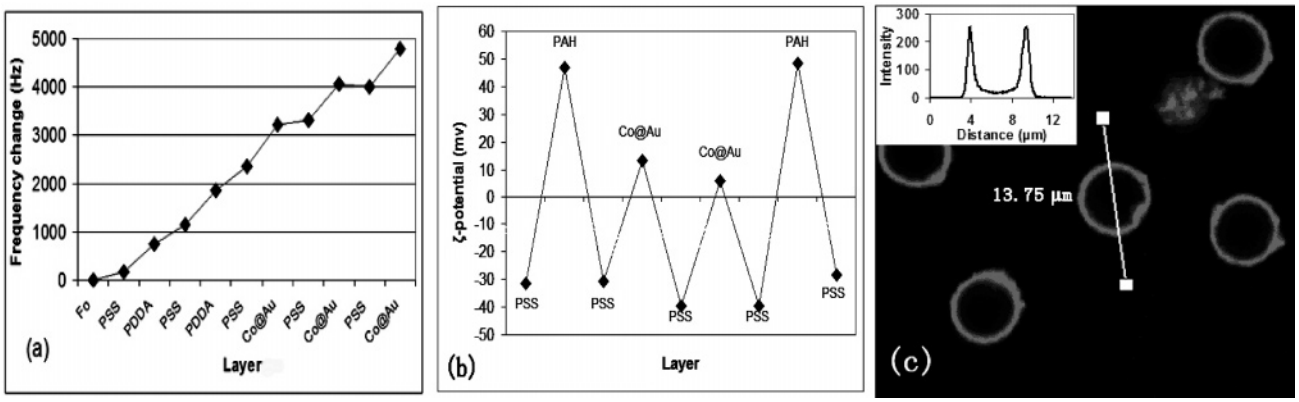

Figure 3. (a) Frequency change of a 9 MHz QCM resonator by alternating adsorption of Co@Au nanoparticles with PSS polymer. (b) Zeta potential changes by alternating adsorption of Co@Au with PSS on $MnCO_3$ cores. (c) Confocal image of RBITC-labeled microcapsules with one layer of embedded Co@Au. The capsule structure is $(PSS/PAH)_4(PSS/Co@Au)_1(PSS/PAH)_6$.

scaling.[16] This value is consistent with the particle diameter obtained from transmission electron microscopy (Figure 2).

After elaboration of the assembly on planar QCM resonators, a similar nanocomposite shell was assembled on manganese carbonate microcores: 4 bilayers of PSS/PAH + 1−2 layers of nanoparticles + 2−10 bilayers of PSS/PAH to cover the nanoparticles. The layers were prepared in aqueous solution with suspended $MnCO_3$ cores as mentioned in the Experimental Section. The final capsule wall composition is $(PSS/PAH)_4(PSS/Co@Au)_{1-2}$-$(PSS/PAH)_{2-10}$. These capsules were used to evaluate their permeability changes under an external alternating magnetic field in the next sections. The influence of the capsule structure differences on the capsule permeability was also investigated. Figure 3b shows the zeta potential changes for Co@Au layers alternated with PSS on $MnCO_3$ microcores. First, we have regular alternation of surface potential with $+45 \pm 5$ mV for PAH and -30 ± 5 mV for PSS. After assembling one layer of Co@Au nanoparticles, the surface charge became positive, +14 mV, and the next PSS layer reverses it to negative, −40 mV. Then, again +8 mV for Co@Au and −42 mV for PSS. This is consistent with the general rule of LbL assembly based on alternation of the surface charge after every deposition step.[1]

After formation of the shells, the template cores were dissolved and hollow microcapsules were obtained, which were studied using confocal and atomic force microscopy. Figure 3c shows the image of the fluorescently labeled magnetic capsules under CLSM; the average capsule diameter is about 5.5 μm. The capsules were labeled with RBITC dye. The fluorescence emitting wavelength of the dye is ∼580 nm under CLSM. This allows us to clearly see the capsule walls outlined in a red color. The capsule wall surface is rather rough with some aggregates, which indicates that more than one monolayer of Co@Au nanoparticles were adsorbed.

AFM study gave us information on the capsule wall thickness with and without magnetic nanoparticles: capsules with a wall composition of $(PSS/PAH)_4(PSS/Co@Au)_1(PSS/PAH)_6$ and similar capsules without Co@Au were dried and checked with AFM. The resulting average wall thickness of the dried magnetic capsules was ca. 500 nm, referring to the thickness of the entire composition of two overlapped capsule walls, including the polyelectrolyte bilayers. This can be compared to the usual microcapsule thickness of 200 nm (overlapped capsule walls composed of 10 polyelectrolyte bilayers without embedded nanoparticles). Therefore, an average thickness of one Co@Au layer on the cores may be estimated as ca. 150 nm. The aggregation of magnetic nanoparticles was considered to be the main contribution of such a large thickness. It is reasonable that we saw aggregation of nanoparticles in our case. Even with charges on their surfaces, particles in the nanoscale have a tendency to aggregate due to their large surface area, high interfacial energy, and hydrophobic effects,[29] especially for magnetic nanoparticles such as Co@Au because they tend to agglomerate more due to their magnetic interactions.

SEM images in Figure 4 visually show the difference between hollow capsules with and without embedded Co@Au nanoparticles. One can see a structured surface of magnetic microcapsules as compared with smoother and thinner nonmagnetic capsules (10 bilayers of PSS/PAH form the walls). The dried capsules without Co@Au nanoparticles are rather thin, with smooth surfaces. Some wrinkles indicate the folding of capsule walls during drying. Figure 4b shows the morphology of dried capsules embedded with one layer of Co@Au nanoparticles. The average capsule diameter is about 6 μm with a thickness of ca. 0.5 μm; this is consistent with the AFM results. The bulges on the capsules also indicate the aggregation of Co@Au nanoparticles during LbL assembly. This is different from LbL assembly of nanoparticles on a planar surface like QCM resonators where an overall growth step for Co@Au nanoparticles was 5 ± 1 nm. We assume that drying of the sample on QCM resonators produces better layer organization due to capillary force ordering.[17] These aggregates increased the amount of Co@Au adsorbed on the capsule walls and resulted in a rougher topology of the magnetic microcapsules.

Magnetic Field Modification of Capsule Permeability. It is assumed in our work that the alternating electromagnetic field influences the Co@Au nanoparticles embedded in the capsule walls. Because the Co@Au particles are ferromagnetic, the oscillating magnetic field will twist and shake the nanoparticles with a frequency corresponding to the frequency of the applied field. This particle agitation will disturb the structure of the surrounding polyelectrolyte layer, which will result in layer structure distortion (some theoretical estimations of corresponding processes are given in the next section). This may result in loosening of the capsule walls and will allow macromolecules to diffuse through the capsule walls.

(28) (a) Sobolev, V. L., et al. *Chin. J. Phys.* **1993**, *31*, 403−419. (b) Comstock, R. L. *Introduction to Magnetism and Magnetic Recording*; Wiley: New York, 1999; pp 1−130. (c) Meiklejohn, W. H., et al. *Phys. Rev.* **1957**, *105*, 904−913.

(29) Myers, D. In *Surfaces, Interfaces, and Colloids*: *Principles and Applications*, 2nd ed.; John Wiley & Sons: New York, 1999; Chapter 10.

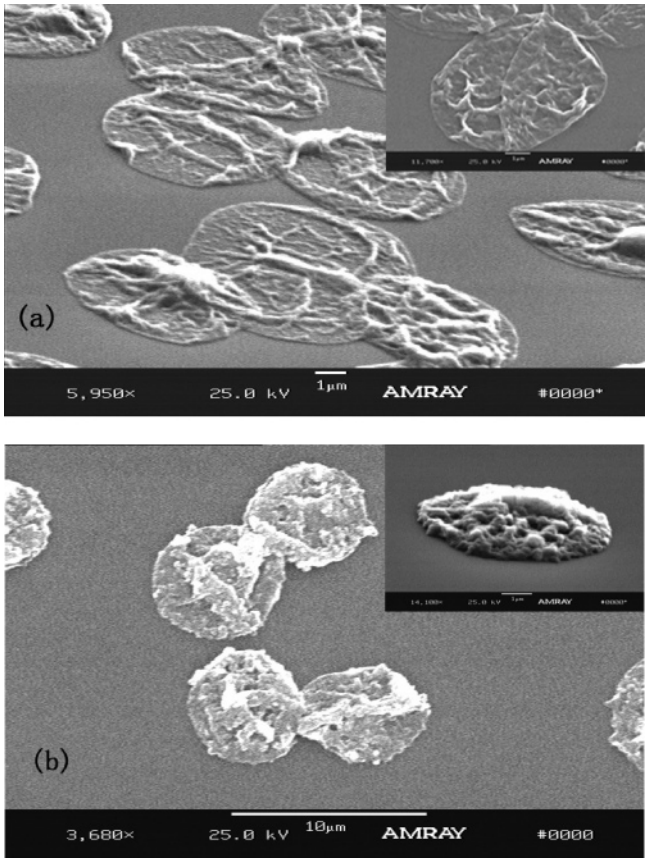

Figure 4. (a) SEM image of hollow capsules with $(PSS/PAH)_{11}$ and (b) SEM image of magnetic capsules with one layer of embedded Co@Au $[(PSS/PAH)_4(PSS/Co@Au)_1(PSS/PAH)_6]$ (both in a dry, collapsed state).

Thus, the permeability of the magnetic microcapsules may be "switched" after applying an alternating magnetic field with relatively low frequencies. We believe we may be able to greatly increase the "switching" rate by finding the resonant frequency of the capsule structure and applying an alternating magnetic field at this resonant frequency.

In our experiments, confocal microscopy was used to check the capsule permeability changes under an alternating magnetic field. Before the experiment, the pH value of the capsule suspension was adjusted to about 7.5 to ensure the capsule walls were in a close, nonpermeable state.[5b,6] To check the permeability, FITC-labeled dextran (MW 2 000 000, pH 7.5, 1 mg/mL) was added to the capsule suspension by 1:1 volume ratio. Figure 5a shows the capsule/FITC−dextran mixture confocal image before applying an alternating magnetic field. The capsules with a wall structure of $(PSS/PAH)_4(PSS/Co@Au)_1(PSS/PAH)_6$ were investigated here. The interior of the capsules is dark even after 1 h of mixing. From the fluorescence intensity profile shown in the image, one can see no FITC−dextran diffused into the capsules after 1 h of incubation; the average fluorescence intensity ratio inside and outside of the capsules is less than 0.2 ($I/I_0 = 0.2$). Therefore, the permeability of the capsules before applying alternating magnetic fields is negligible, and FITC−dextran was blocked from diffusion into the capsules. After applying an alternating electromagnetic field (1200 Oe, 150 Hz) to the capsule/FITC−dextran mixture for 30 min, the capsules became permeable (Figure 5b). The image shows that the fluorescence intensity inside the capsules became the same as in bulk solution, and the average fluorescence intensity ratio inside and outside of the capsules is about 1.1 ($I/I_0 = 1.1$), which proves there is a large enhancement of FITC−dextran diffusion into the capsules. The fluorescence intensity in the capsule walls is much higher because the capsule walls are constructed from charged polyelectrolytes, which adsorb more FITC−dextran than the interior of the capsules. By checking the capsules using CLSM, 99% of the capsules analyzed were filled with FITC−dextran after applying an alternating magnetic field for 30 min. The same permeability experiments were run four separate times with similar results. The experimental results supported the assumption that a low-frequency alternating magnetic field changes the permeability of magnetic capsules, allowing the macromolecules, which are usually excluded from the capsules, to penetrate into the capsules. The permeability control mechanism is given in more detail in the theoretical considerations section.

Another part of our work had to do with moving and focusing the magnetic microcapsules with a permanent external magnetic field (~3 kG). This was done first by placing a permanent magnet near the Co@Au nanoparticles suspended in DI water. After 5 min, all the nanoparticles migrated to the magnet and the bulk solution turned from a murky color to transparent. Then, similar experiments were done with capsules embedded with Co@Au nanoparticles with analogous results. This shows that the microcapsules embedded with Co@Au nanoparticles can be concentrated using a permanent magnet. Therefore, we may suggest any one approach, both "focusing" of the capsules to a specific location followed by "switching" them to release their contents.

Temperature, Frequency, and Layer Composition Optimization. During the application of an alternating magnetic field, we observed a 10−20 °C increase in temperature for the sample as is shown in Figure 6a. Therefore, we have to separate the two phenomena possibly contributing to the changing of the polyelectrolyte wall permeability: heating of the sample and disturbing of the capsule walls. From the literature,[3] it is known that heating provides an opposite effect, decreasing wall permeability. Even so, we designed an experiment to rule out the temperature influence on the capsule permeability. In this experiment, magnetic capsules were mixed with FITC−dextran and heated to 50 °C for 30 min (which were typical conditions when applying a magnetic field). The permeability was checked (Figure 6b), and the capsules were found not to be permeable; the FITC−dextran remained excluded from the capsules even after 30 min and longer, and the average fluorescence intensity ratio inside and outside of the capsules (I/I_0) is less than 0.2. Thus, one can conclude that the temperature's influence on the permeability of capsules is negligible and even may oppose the magnetic effects; the influence of magnetic fields is the major factor contributing to the capsule permeability change.

The influence of frequencies of electromagnetic fields on the permeability of capsule walls was also studied. The applied frequencies ranged from 100 to 1000 Hz, while the strength of the magnetic field was kept constant at 1200 Oe. For frequencies beyond 300 Hz, the diffusion of FITC−dextran into capsules is negligible, even after keeping the mixture for 1 h in the magnetic field. For frequencies less than 300 Hz, there is a tendency for faster diffusion of FITC−dextran with lower frequencies. It seems that the increase of frequency reduces agitation effects of the magnetic field on the Co@Au nanoparticles embedded in the capsule walls, which reduces the permeability of the magnetic capsules. This is consistent with our idea that agitating magnetic forces have to correspond

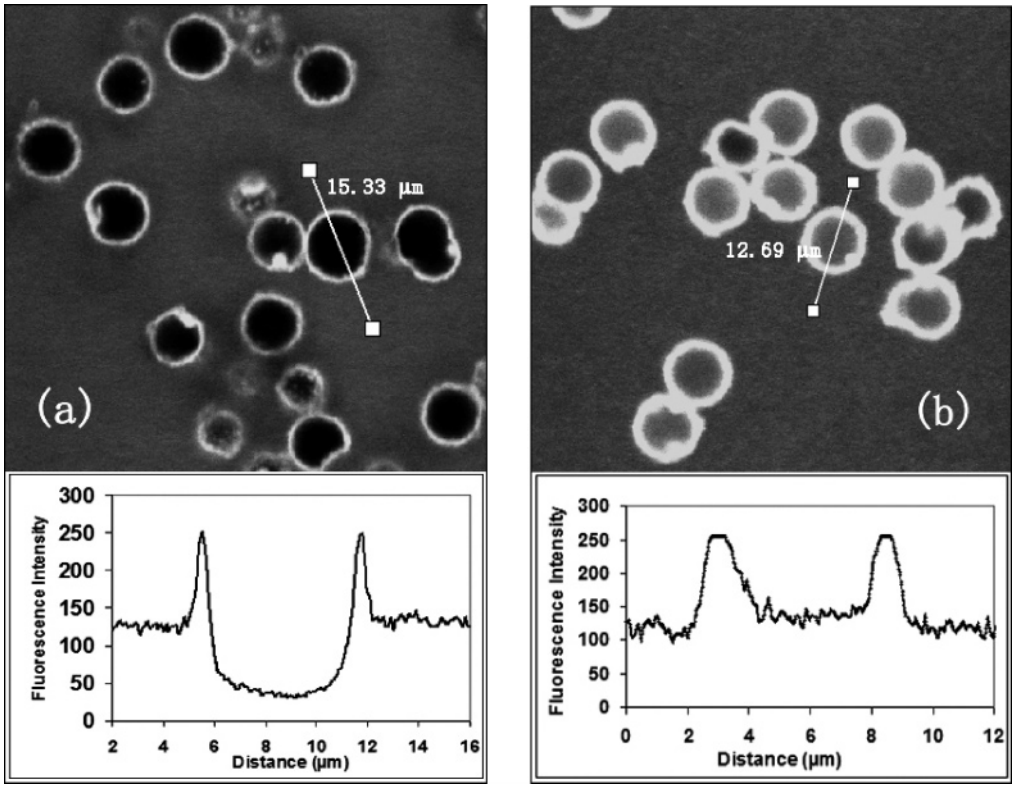

Figure 5. CLSM image of magnetic capsules [$(PSS/PAH)_4(PSS/Co@Au)_1(PSS/PAH)_6$] mixed with FITC−dextran (a) without applying an alternating magnetic field for 1 hour and (b) after applying an alternating magnetic field for 30 min. The corresponding optical density profiles are also shown.

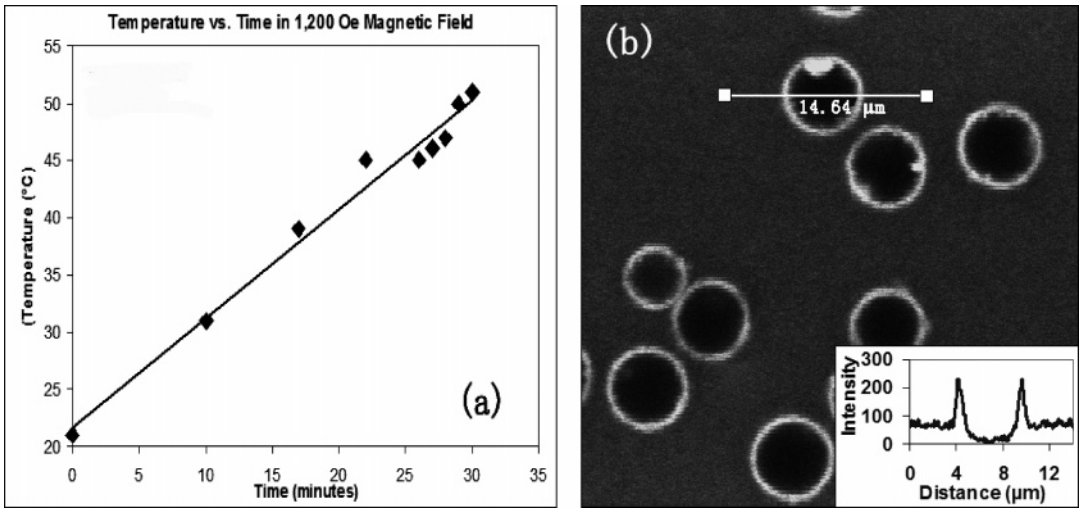

Figure 6. (a) Temperature increase tendency of the capsule suspension when applying a magnetic field. (b) CLSM image of the magnetic capsule [$(PSS/PAH)_4(PSS/Co@Au)_1(PSS/PAH)_6$]/FITC−dextran mixture after heating to 50 °C for 30 min.

with mechanical properties of the magnetic particles and surrounding elasticity. Our search of a resonant frequency, which may drastically enhance the effect, is in progress.

Optimization of the Capsule Wall Composition. The increase in the number of Co@Au nanoparticle layers significantly reduced the permeability of the capsules. After coating two layers of Co@Au nanoparticles, the capsules were not permeable to FITC−dextran in any case; therefore, the use of more than one layer of Co@Au nanoparticles is unsuitable for our experiments. The influence of the number of PSS and PAH layers on capsule permeability was also investigated. The permeability change of the capsules was evaluated using the fluorescence intensity ratio inside and outside the capsules after adding FITC−dextran into the capsule suspension as the above section described. The line with triangle markers in Figure 7 shows the permeability change tendency with changes in the number of polyelectrolyte bilayers for capsules without embedded nanoparticles. The capsules with less than 4 bilayers are easily permeable to FITC−dextran ($I/I_0 > 0.9$). The permeability is gradually reduced as the number of bilayers is increased, and the capsules are totally impermeable to FITC−dextran with more than 8 bilayers ($I/I_0 < 0.1$). The line with square markers in Figure 7 shows the permeability changes of capsules with one layer of embedded Co@Au nanoparticles. The permeability of the magnetic capsules is enhanced when compared to that of the capsules without nanoparticles, but the general behavior is the same. It was also found that, in an alternating electromagnetic field, the mag-

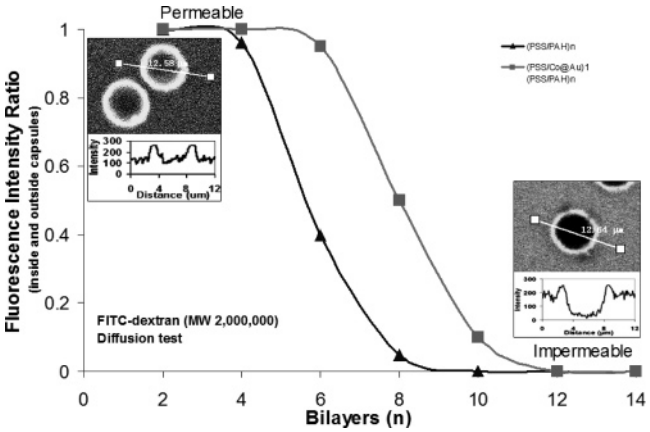

Figure 7. Influence of polyelectrolyte bilayer numbers on the permeability of capsules with and without an embedded layer of Co@Au nanoparticles at pH 7.5 (no magnetic field applied).

netic capsules will not be open for FITC−dextran if more than 12 polyelectrolyte bilayers (PSS/PAH) are assembled.

Theoretical Considerations. It is easy to show that ideal isolated hcp (hexagonal-close packed) Co nanoparticles, with a diameter of ~3 nm, should be superparamagnetic at room temperature with blocking temperature $T_B \sim 4$ K from the equation

$$T_B \sim KV/25k_B \quad (1)$$

where $K \sim 10^6$ erg/cm^3 (anisotropy constant), V is the particle volume, and k_B is the Boltzmann constant. Such nanoparticles should have a very low magnetic moment at room temperature in reasonable magnetic fields. In reality, the situation is even worse because it is difficult to expect perfect crystallinity for particles of 3 nm in diameter. Moreover, in our case partial oxidation of cobalt takes place. A typical shift of the hysteresis loop along the H axis for nanoparticles cooled to 30 kOe due to unidirectional anisotropy, which is a result of the formation of an oxide layer,[27c] was observed (Figure 2c). The oxidation should also decrease the magnetic moment of the nanoparticles. However, magnetic data obtained for dried, as-prepared Co@Au nanoparticles show that they behave as typical ferromagnetic materials (Figure 2d). The only possible explanation of this fact is aggregation of the Co@Au nanoparticles. Due to the magnetostatic interaction between nanoparticles, aggregations became ferromagnetic. Correlation of magnetic moments of chaotically oriented particles leads to a fairly narrow hysteresis loop at room temperature (Figure 2c). Thus the resulting volume of the aggregates should be at least a hundred times the volume of the individual nanoparticles (i.e., the diameter of the aggregate would be at least 6 times larger than that of the Co@Au nanoparticle). These aggregates play a major role in the permeability of polyelectrolyte microcapsules under the application of an alternating magnetic field.

Let us consider the action of alternating magnetic fields on polyion capsules with embedded Co-ferromagnetic nanoparticles. There are several mechanisms, which can lead to formation stresses inside of the shell. One such mechanism is that the deformation of the capsule could lead to a decrease of the viscous interaction due to a decreasing cross-sectional area. However, we cannot expect considerable gradients of the magnetic field ($\delta H/\delta x$). The magnetic force, $F = MV(\delta H/\delta x)$, where M is the mean magnetization of the capsule and V is the volume, will be negligible. Another mechanism is that the capsule in the magnetic field tried to stretch itself along the field direction because it leads to a decrease of magnetostatic energy,

$$E_{ms} = 1/2(N_{||} - N_{\perp})M^2V \quad (2)$$

where $N_{||}$ and $N_{\perp}$ are demagnetizing factors in the directions parallel and perpendicular to the magnetic field. Taking into account real physical parameters of the capsules, one can show that the influence of this should also be negligible.[18−19] Besides, the increase of the thickness of the nanoparticle layer in this case would lead to an increase of the influence of the magnetic field.

Shape and magnetocrystalline anisotropy of individual nanoparticles also cannot affect the permeability of the capsules. The arising forces will be too low for substantial deformation of the capsule walls. However, this is not the case for aggregations of nanoparticles. Magnetostatic interactions inside the aggregations will lead to an appearance of fairly large demagnetizing fields. In a magnetic field, they will try to align their easy axis along the direction of the magnetic field. This results in the formation of rather large stresses inside the capsule walls. Such stresses can lead to an increase of pore size in the capsule walls, and in some cases even rupture the walls. All this speculation is true for separated aggregates; otherwise, magnetostatic interactions between the aggregates would suppress the demagnetizing factors of the individual aggregates.[19]

As for the frequency behavior of the permeability, the aggregates rotate, or oscillate, under the action of the magnetic field with the elastic deformation of the capsule walls. At high frequencies, they will not follow the variation of the magnetic field and the deformation will be minimal, which leads to a decrease in permeability. This corresponds to the forced oscillation of a pendulum at frequencies above the resonance frequency. Unfortunately, it is impractical to calculate theoretically elastic forces for such a complex system and eigen-frequencies could be determined from experiment only.

Conclusion

The synthesized 3 nm diameter ferromagnetic Co@Au nanoparticles are positively charged in DI water (~pH 7) and can be successfully absorbed on planar and spherical surfaces in alternation with anionic polyelectrolyte layers. Also, 5.5 μm diameter microcapsules with nano-organized polymer walls embedded with Co@Au nanoparticle layers were successfully fabricated. They form a stable aqueous dispersion. Applying external alternating electromagnetic fields of 100−300 Hz and 1200 Oe strength disturbed the capsule wall structures and drastically increased their permeability to macromolecules. Capsules with 1 layer of Co@Au nanoparticles and 10 polyelectrolyte bilayers are considered optimal for controlling permeability with alternating magnetic fields. This work supports our hypothesis of using magnetic nanoparticles embedded in polyelectrolyte capsules for controlled release of substances and offers a promising technology for microcapsule "focusing" and "switchable" drug release in the biomedical studies by using an external magnetic field to displace and open the capsules at designated places within the body.

Acknowledgment. We thank Professor Elizabeth Podlaha for support in magnetic nanoparticle preparation and testing and Professor Joseph Hormes, both of Loui-

siana State University, Baton Rouge, for encouragement. We are thankful to Professor L. L. Henry of Southern University, Baton Rouge, for making available SQUID measurements. This work is partially supported by NSF No. 0210298, NIH-1RO1 EB00739-01, and DARPA-MDA 972-63-C-0100 grants. Any opinions, findings, and conclusions or recommendations expressed in this material are those of the authors and do not necessarily reflect the view of the National Science Foundation. Support of the Louisiana Board of Regents with Grant 2002-RDA-19 is acknowledged.

LA047629Q